

Prostate-Specific Genes and Their Regulation by Dihydrotestosterone

Ma Ci, Yoshioka Mayumi, Boivin André, Belleau Pascal, Gan Lin, Takase Yasukazu, Labrie Fernand, and St-Amand Jonny*

Molecular Endocrinology and Oncology Research Center, Laval University Medical Center, Department of Anatomy and Physiology, Laval University, Québec, Canada

BACKGROUND. Prostate is a well-known androgen-dependent tissue.

METHODS. By sequencing 4,294,186 serial analysis of gene expression (SAGE) tags, we have investigated the transcriptomes of normal mouse prostate, liver, testis, lung, brain, femur, skin, adipose tissue, skeletal muscle, vagina, ovary, mammary gland, and uterus in order to identify the most abundant and tissue-specific transcripts in the prostate, as well as to target the androgen responsive transcripts specifically regulated in the prostate. Small interference RNA (siRNA) in LNCaP cells was applied to validate the roles of prostate-specific/enriched ARGs in the growth of human prostate cancer cells.

RESULTS. The most abundant transcripts were involved in prostatic secretion, energy metabolism and immunity. Previously well-known prostate-specific transcripts, including many transcripts involved in prostatic secretion, polyamine biosynthesis and transport, and immunity were specific/enriched in the prostate. Only 22 transcripts among 114 androgen-regulated genes (ARGs) in the mouse prostate were modulated by dihydrotestosterone (DHT) in two or more tissues. The siRNA results showed that inhibition of HSPA5 and MAT2A gene expression repressed growth of human cancer LNCaP cells.

CONCLUSIONS. The current study globally assessed the transcriptome of the prostate and revealed the most abundant and tissue-specific transcripts which are responsible for the unique functions of this organ. These prostate-specific ARGs might be used as targets to develop safe and effective gene-based therapy for the prevention and treatment of prostate cancer. *Prostate* 68: 241–254, 2008. © 2007 Wiley-Liss, Inc.

KEY WORDS: serial analysis of gene expression; androgen-regulated genes; mRNA; prostate cancer

INTRODUCTION

The prostate is the largest male accessory gland and is generally known as an exocrine gland. The main function of the mammalian prostate gland is to enhance fertility by secreting buffers, proteins and protective agents that maintain sperm in a quiescent and intact state as they pass through the male reproductive tract [1]. In addition to its physical contribution in the control of urine output from the bladder and in the transmission of seminal fluid during ejaculation, prostate also functions as an endocrine gland, rapidly metabolizing testosterone to the more potent androgen, dihydrotestosterone (DHT), and thus influencing both hypothalamic and hypophyseal functions [2]. Despite some anatomical differences between rodents and humans, these organisms share essential similarities.

Studies of the mouse prostate undoubtedly offer valuable information for human prostate.

Genomic expression profiling enables the determination of the repertoire of expressed genes and their corresponding level of expression in a given tissue. Thus, it offers knowledge of the general and unique functions of the tissue. Serial analysis of gene expression (SAGE) is a powerful strategy which can

*Correspondence to: St-Amand Jonny, PhD, Director, Functional Genomics Laboratory, Molecular Endocrinology and Oncology Research Center, Québec Genome Center, Laval University Medical Center (CHUL), 2705 Boul. Laurier, Québec, Canada G1V 4G2.

E-mail: jonny.st-amand@crchul.ulaval.ca

Received 29 June 2007; Accepted 23 October 2007

DOI 10.1002/pros.20712

Published online 19 December 2007 in Wiley InterScience

(www.interscience.wiley.com).

accurately measure the expression of thousands of genes, including novel transcripts [3,4]. There is a general assumption that the most abundant transcripts encode various ribosomal proteins, translation factors and housekeeping genes in all tissues and organs including prostate. However, using the SAGE method, we have recently shown that the most abundant mRNA species are sufficiently specific to identify various tissues such as skeletal muscle [5,6], uterus [7], brain [8], and adipose tissue [9,10]. For instance, in the skeletal muscle, transcripts involved in energy metabolism and the contractile apparatus, involved in unique functions of this organ, were the most abundantly expressed [5,6]. Since the prostate is generally known as an exocrine gland which secretes small molecules, protein and nutrients that contribute to the seminal plasma, enhancing spermatozoa motility [2], we hypothesize that prostate may synthesize mRNA species involved in these unique functions in preference to other transcripts. In order to characterize the normal prostate transcriptome, we identified the most abundant transcripts using SAGE. In addition, we generated a number of SAGE expression profiles, including prostate, liver, testis, lung, brain, bone, skin, adipose tissue, skeletal muscle, vagina, ovary, mammary gland, and uterus to identify prostate tissue-specific genes. A previous study has shown prostate tissue-specific transcripts with 50,562 expressed sequenced tags (EST) corresponding to 15,009 transcript species and suggested a potential role for the prostate as a defensive barrier for entry of pathogens into the genitourinary tract [11]. In the current study, we sequenced 142,886 SAGE tags corresponding to 46,738 transcript species in the prostate and a total of 1,848,322 SAGE tags in the other normal tissues. Our wide analysis verified the conclusion of the previous studies and suggests that, in addition to the prostatic secretion, the prostate has unique roles in polyamine biosynthesis and transport as well as immunity.

Prostate is well known to be a highly androgen-dependent tissue. Moreover, androgen plays very important roles in the development of prostate disease states such as benign hyperplasia and cancer. Although the specific mechanisms by which androgens alter cellular growth in these conditions remain to be delineated, investigating androgen-regulated genes (ARGs) in normal/benign prostate should extend our knowledge on prostate physiology and elucidate the influence of androgens on prostate differentiation and transformation to adenocarcinoma. We have already shown the effect of DHT, the most potent androgen, on global gene expression in this organ [12]. In the current study, we compared several DHT-treated tissues including adipose tissue, skeletal muscle, uterus and

mammary gland, and identified the common ARGs which could be common regulators of DHT effects. For example, DHT and testosterone are clinically used to prevent muscle atrophy and weakness, and to treat sexuality and fertility impairments [13]. The information of common and prostate-specific ARGs may be useful in efforts to retain the beneficial effects and avoid side effects of DHT. Thus, the current study provides valuable references for safe and effective gene-based and hormonal therapies for the prevention and treatment of benign prostatic hyperplasia and prostate cancer.

MATERIALS AND METHODS

Sample Preparation

Prostate tissue was obtained from 51 male C57BL6 mice, 10–12 weeks old, for the intact group, and from 14 mice per group for gonadectomy (GDX) and GDX + DHT treatment. Other tissues were obtained from at least 10 intact mice: liver (n = 24), testis (n = 24), lung (n = 24), brain (n = 51), femur (n = 24), skin (n = 25), male adipose tissue (n = 10), male skeletal muscle (n = 26), female skeletal muscle (n = 25), female adipose tissue (n = 25), vagina (n = 50), ovary (n = 50), mammary gland (n = 14), and uterus (n = 50). For the GDX and GDX + DHT treatments, adipose tissue, skeletal muscle, uterus and mammary gland were sampled from at least 10 mice. The animals were purchased from Charles River, Québec, Canada, Inc. and had free access to Lab Rodent Diet No. 5002 (Ren's Feed and Suppliers, Ontario) and water. GDX was performed 7 days prior to organ collection for GDX and GDX + DHT groups. DHT (0.1 mg) was injected 3 hr (DHT3h) and 24 hr (DHT24h) prior to sacrifice in the DHT groups. The control group (GDX) received vehicle solution (0.4% (w/v) Methocel A15LV Premium/5% ethanol) 24 hr prior to sacrifice. All animal experimentation was conducted in accord with the requirements of the Canadian Council on Animal Care. Each tissue from all mice of the same group was pooled to eliminate inter-individual variations and to extract sufficient amount of mRNA. The tissues were stored at -80°C until RNA extraction.

Transcriptome Analysis

The SAGE method was performed as previously described [3,5,14,15]. Polyadenylated RNA was extracted, annealed with the biotin-5'-T₁₈-3' primer and converted to cDNA using a cDNA synthesis kit (Invitrogen, Carlsbad, CA). The resulting cDNA library was digested with *Nla*III (anchoring enzyme) and the 3' restriction fragments were isolated with

streptavidin-coated magnetic beads (Dynal Biotech, Oslo, Norway) and separated into two populations. Each population was ligated to one of the two annealed linker pairs and extensively washed to remove unligated linkers. The tag beside the most 3' *Nla*III restriction site (CATG) of each transcript was released by digestion with *Bsm*FI (tagging enzyme). The blunting kit from Takara Co. (Kyoto, Japan) was used for the blunting and ligation of the two tag populations. The resulting ligation products containing the ditags were amplified by PCR with an initial denaturation step of 1 min at 95°C followed by 22–26 cycles of 20 sec at 94°C, 20 sec at 60°C and 2 sec at 72°C using 27 bp primers [5,8–10]. The PCR product was then digested with *Nla*III and the band containing the ditags was extracted from a 12% acrylamide gel. The purified ditags were self-ligated to form concatemers. The concatemers ranging from 500 to 1,800 bp were isolated by agarose gel electrophoresis. The resulting DNA fragments were ligated into the *Sph*I site of pUC19 and cloned into UltraMAX DH5 α FT (Invitrogen). White colonies were screened by PCR to select long inserts for automated sequencing. Approximately 150,000 tags were sequenced in each library of prostate, liver, lung, brain, skin, skeletal muscle, uterus and female adipose tissue, and approximately 50,000 tags were sequenced in each library of testis, femur, vagina, ovary, male adipose tissue, and mammary gland. The data were normalized to 100,000 tags for presentation.

Bioinformatic Analysis

Sequence files were analyzed using the SAGEana program, a modification of SAGEparser [4]. Tags corresponding to linker sequences were discarded and duplicate concatemers were counted only once. Identification of the transcripts was obtained by matching the 15 bp (CATG + 11 bp tags) with UniGene and GenBank databases. The matching procedure used was very restrictive since in order to avoid the possibility of sequencing errors in the EST database; we did not consider the matches that were identified only once among the numerous sequences of a UniGene cluster. Indeed, the possibility of matches with EST containing sequencing errors drops dramatically when at least two EST are identified in a UniGene cluster for a given tag sequence. A minimum of one EST with a known polyA tail had to be in the UniGene cluster to identify the last *Nla*III site on the corresponding cDNA. Classification of the genes was based upon the updated information of the genome directory [16] found at the TIGR web site (<http://www.tigr.org/>).

The probability of signal peptide was analyzed by using the SignalP 3.0 program (<http://www.cbs.dtu.dk/services/signalp/>).

Cell Culture and Small Interfering RNA (siRNA) Transfection

Androgen-sensitive human prostate cancer (LNCaP) cells were purchased from the American Type Culture Collection (ATCC, Manassas, VA). They were maintained in phenol red-free RPMI-1640 medium (Fisher Scientific, Ottawa, Canada) supplemented with 10% (v/v) fetal bovine serum (FBS) (Wisent, Inc., St-Bruno, Canada) and antibiotics (100 U/ml penicillin and 100 μ g/ml streptomycin) (Sigma–Aldrich Canada Ltd., Oakville, Canada) at 37°C under 95% air–5% CO₂ humidified atmosphere.

LNCaP cells were seeded at 3×10^5 cells/well on poly-L-lysine (Sigma–Aldrich Canada Ltd.) treated 6-well cell culture plates with phenol red-free RPMI-1640 medium supplemented with 10% FBS and antibiotics, and were allowed to adhere for 48 hr. The cells were transiently transfected using LipofectamineTM 2000 (Invitrogen) in Opti-MEM[®] I Reduced Serum Medium (Invitrogen), according to the manufacturer's instructions. Briefly, 80 nM negative control, two target StealthTM RNAi oligos (Invitrogen) were transfected into the LNCaP cells for 24 hr, and then the medium was replaced with fresh steroid-reduced medium (phenol red-free RPMI-1640 medium supplemented plus 5% charcoal-stripped FBS (Wisent) and antibiotics) with 10 pM R1881 for 72 hr. Mock treatment was performed with LipofectamineTM 2000 alone. The GenBank accession numbers (positions) used for the sense sequences of target siRNA oligos were NM_005911.2 (221–245) for methionine adenosyltransferase II alpha (MAT2A) and NM_005347.2 (1732–1756) for heat shock 70 kDa protein 5 (HSPA5).

A cell proliferation assay was performed 96 hr after the transfection by measuring DNA contents with diaminobenzoic acid (DABA) (Sigma–Aldrich Canada Ltd.). In brief, medium was removed and remaining cells were fixed with 500 μ l methanol per well. The 450 μ l of filtered DABA solution (90 ml of 4N HCl (Fisher Scientific), 20 g of DABA and 10 g of carbon (Fisher Scientific) was added in each well, and incubated for 60 min at 60°C. After placing the plate on ice, 3.75 ml of 1N HCl was added in each well. The absorbance at 400 nm (excitation) and 508 nm (emission) was recorded with plate reader (Fluorolite 100, Opti-Ressources, Inc., Charny, Canada). The DNA contents were calculated using DNA standards (MP Biochemical, Montreal, Canada).

Cell cycle analysis was also performed, at 96 hr after the transfection, with flow cytometry by staining cells with propidium iodide (PI) (Sigma–Aldrich Canada Ltd.). In detail, medium containing cells were transferred to 5 ml tube and centrifuged for 5 min at 2,000 rpm. The cells were washed twice with 2 ml of phosphate buffer

solution (PBS) (Invitrogen), in which 0.8 ml was used for following cell cycle analysis and cells in 1.2 ml were collected, frozen with liquid N₂ and stored at -80°C for quantitative real-time PCR (Q_RT-PCR) analysis. The sample for cell cycle analysis was centrifuged for 5 min at 2,000 rpm and cells were re-suspended in 0.3 ml PBS. The 0.7 ml ice-cold ethanol (Fisher Scientific) was added and stored at -20°C for overnight. After washing cells with 3 ml PBS, cells were re-suspended in 250 µl of PI staining solution (5 ml of 0.1% Triton X-100 in PBS (Sigma-Aldrich Canada Ltd.), 250 µl of 1 mg/ml PI and 2 mg DNase-free RNase A (Sigma-Aldrich Canada Ltd.), and incubated at 37°C for 30 min. The tube was placed on ice until analysis with EPICSXL set at 488 nm and System II Software (Beckman Coulter Canada, Inc., Mississauga, Canada). The mRNA expression of the target genes and interferon response at 96 hr after the transfection was evaluated by the Q_RT-PCR.

Q-RT-PCR

First-strand cDNA was synthesized using isolated total RNA in a reaction containing 200 U of Superscript III RNase H-RT (Invitrogen), 300 ng of oligo-dT₁₈, 500 mM deoxynucleotides triphosphate, 5 mM dithiothreitol and 34 U of human RNase inhibitor (Amersham Pharmacia, Piscataway, NJ) in a final volume of 50 µl. The reaction was performed at 50°C for 2 hr and then treated with RNase A for 30 min at 37°C. The resulting products were purified with Qiaquick PCR purification kits (Qiagen). The cDNA corresponding to 20 ng of total RNA was used to perform fluorescent-based RT-PCR quantification using the LightCycler RT-PCR apparatus (Roche, Inc., Nutley, NJ). Reagents were obtained from the same company and were used as described by the manufacturer. The conditions for PCR reactions were: denaturation at 95°C for 10 sec, annealing at 56–66°C for 5 sec and elongation at 72°C for 7–13 sec. The reaction was then heated for 3 sec at 2°C lower than the melting temperature of the DNA fragment. Readings of the fluorescence signal were taken at the end of the heating to avoid non-specific signal. A melting curve was performed to assess non-specific signal. Oligoprimers that allow the amplification of approximately 200 bp were designed by GeneTools software (Biotools, Inc., Edmonton, AB) and their specificity was verified by blast in GenBank database. The GenBank accession numbers (regions) used for the primer pairs were NM_005347 (1,933–2,125) for HSPA5, NM_005911 (1,969–2,204) for MAT2A, NM_001547 (1,645–1,914) for interferon-induced protein with tetratricopeptide repeats 2 (IFIT2), and NM_001549 (1,261–1,489) for IFIT3. Data calculation and normalization was performed using second

derivative and double correction method using the housekeeping gene hypoxanthine guanine phosphoribosyl transferase 1 [17]. The expression levels of mRNA are expressed as number of copies/µg total RNA using a standard curve of crossing point (Cp) versus logarithm of the quantity. The standard curve was established using known cDNA amounts of 0, 10², 10³, 10⁴, 10⁵, and 10⁶ copies of hypoxanthine guanine phosphoribosyl transferase 1 and a LightCycler 3.5 program provided by the manufacturer (Roche, Inc.). All measurements were performed in triplicate on three unique samples. The values of HSPA5 and MAR2A gene expression were expressed as a ratio to the negative control siRNA oligo.

Statistical Analysis

The comparative count display (CCD) test was used to identify transcripts that were differentially expressed significantly ($P \leq 0.05$) between groups with more than a twofold change [18]. The CCD test was applied for comparison of groups of different tissues as well as different treatments. The data are normalized to 100,000 tags in order to facilitate visual comparison in the tables.

For the siRNA experiments, one-way ANOVA test with Fisher PLSD post hoc test or *t*-test was used to determine statistical significance between groups ($P \leq 0.05$).

RESULTS

A total of 142,886 tags were sequenced in the prostate gland of intact mice, which corresponded to 46,738 tag species. Fifty-nine distinct transcripts were expressed as more than 0.1% of the total mRNA population in the prostate and these tags constituted 27% of mRNA population. Figure 1 shows the functional distribution of these transcripts. As illustrated in Figure 1, prostate plays important roles in many physiological processes including protein secretion (38%), protein expression (4%), energy metabolism (6%), cell/organism defence (1%), cell structure (0.5%) and lipid metabolism (0.5%).

Table I shows the top 20 most highly expressed transcripts in the prostate of intact mice. The most abundant transcripts were involved in prostatic secretion, energy metabolism and immunity.

By comparing 17 SAGE libraries from male and/or female mice (prostate, liver, testis, lung, pituitary, hypothalamus, cerebral cortex, bone, skin, male and female adipose tissue, male and female skeletal muscle, vagina, ovary, mammary gland, and uterus), 79 prostate-specific/enriched transcripts were identified by sequencing a total of 1,950,777 tags (Table II). These transcripts are related to prostatic secretion, polyamine metabolism and immunity. Interestingly, the majority

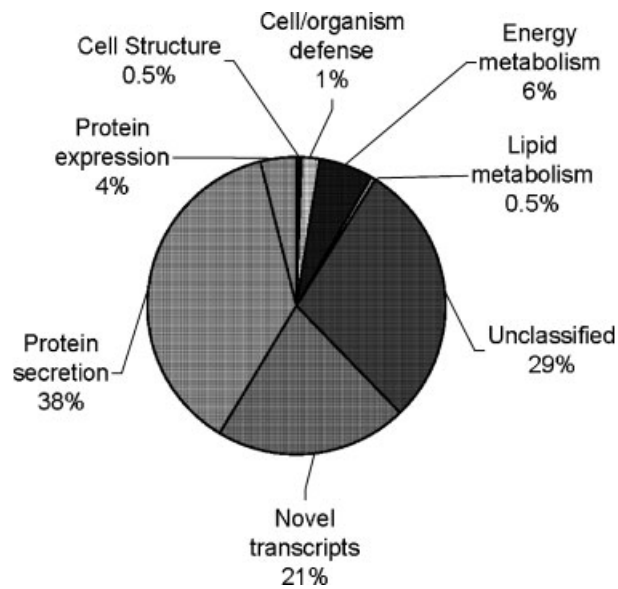


Fig. 1. Functional distribution of the gene expressed at more than 0.1% of the total mRNA population in the prostate.

(14/20) of the top 20 most abundant transcripts were prostate specific (SAGE tag counts in the other tissues are 0 or 1) or enriched (differential expression from the other tissues) compared to other organs. Since prostate is well known to be an androgen-dependent tissue and androgen is necessary for the prostate's physiological roles, the androgen modulation of each transcript was determined. The tag numbers sequenced for GDx, DHT3h and DHT24h were 156,033, 134,831, and 138,403, respectively.

In order to validate the role of tissue-specific ARGs in prostate cancer cell growth, we knocked-down HSPA5 and MAT2A by siRNA in the LNCaP cells and measured mRNA of HSPA5, MAT2A, IFIT2, and IFIT3 as well as cell proliferation and cell cycle at 96 hr after the transfections (Table III). The transfections of HSPA5 and MAT2A siRNAs did not induced any interferon responses. The MAT2A siRNA inhibited MAT2A gene expression by 59% compared to the negative control siRNA. Moreover, MAT2A and HSPA5 siRNAs decreased cell proliferation and

TABLE I. Top 20 Most Abundant Transcripts in Prostate

Tags	Nb	%	Abbr	Description (UniGene, GenBank)	GDxDHT
Protein secretion					
TTCTAATCGGT	1925	1.93	PBSN	Probasin (8034, AF005204)	↓
GCAGCGCCTCC	4727	4.73	SBP	Spermine binding protein (328841, AK009406; 46428, AV089729)	↓
ATGCAGTGGCG	414	0.41	SPINK3	Serine protease inhibitor, Kazal type 3 (272, AK007841)	↓ ↑
CTTGTTTGTCT	1265	1.26	SVP2	Seminal vesicle protein 2 (1286, AK020349)	
AACCAACGATC	380	0.38	SVS2	EST seminal vesicle protein, secretion 2 (143501, BB123697)	↓
GACAACCCTCT	1958	1.96	SVS2	Seminal vesicle protein, secretion 2 (143501, AK035204) and EST RIKEN (227954, BB525728)	
GGCCTAGAAA	2319	2.32	SVS5	Seminal vesicle secretion 5 (140154, NM_009301)	↓ ↑
ATGGCTGAGA	514	0.51	SVS7	Seminal vesicle protein, secretion 7 (99349, AF134204)	↓ ↑
GGAGGTAGACC	614	0.61	TGM4	Transglutaminase 4 (prostate) (195309, AK035279)	↓ ↑
Energy/TCA cycle					
ATAATACATAA	747	0.75	ATP6	ATP synthase F0 subunit 6 (NC_001569, position 8596)	
ATACTGACATT	466	0.47	COX3	Cytochrome c oxidase subunit 3 (NC_001569, position 9325)	
Immunity					
GTACCTGTGAG	532	0.53	DEFB50	Defensin beta 50 (346928, NM_199067)	↓ ↑
Functionally uncharacterized transcript					
CTCACTTAGTG	481	0.48	9530002B09 RIK	RIKEN cDNA 9530002B09 gene (157655, AF319955)	↓
Novel transcripts					
TGCCAACTGAT	1318	1.32		No match	
GTCCTGAGGG	724	0.72		No match	
GATGAAGGTAT	634	0.63		No match	
AGATTTATTTT	628	0.63		No match	
GCAAATCCTTT	361	0.36		No match	
AAAAAGTACCA	342	0.34		No match	
Multiple matches					
GTGGCTCACAA	454	0.45		527 matches	

Nb, tag number normalized to 100,000 tags. %, the relative frequency calculated by dividing the observed tag count by the total count of 142,886 tags sequenced in prostate SAGE library; Abbr, abbreviation; GDx, gonadectomized; DHT, dihydrotestosterone; Arrows show the significant effects of GDx compared to intact group, or DHT compared to GDx group on the gene expression level ($P \leq 0.05$).

TABLE II. Tissue-Specific/Enriched Transcripts in the Prostate and Their Regulation by DHT

Tags	Prostate (142886)	Liver (169988)	Testis (56750)	Lung (159072)	Pituitary (126688)	Hypothalamus (165825)	Cerebral cortex (161045)	Femur (74763)	Skin (160828)	Male Fat (46057)	Male muscle (133398)	Female muscle (117944)	Female fat (150155)	Vagina (50724)	Ovary (55966)	Mammary gland (40411)	Uterus (178688)	Abbr	Description (UniGene, GenBank)	GDx	DHT
Protein secretion																					
TGACAAAACGT	99	1	0	0	0	1	0	0	0	0	0	0	0	0	0	0	0	PSP94/ BMSP	Beta-microseminoprotein (2540, U89840)	↓	
TGGTGTAGGAA	141	37	2	1	2	1	0	0	41	0	1	1	17	0	0	25	56	HSPA5	Heat shock 70kD protein 5 (glucose-regulated protein) (330160, BC050927)		↑S
CCTGGTGAAG	45	0	0	0	0	1	0	0	0	0	0	0	0	0	0	0	0	MUC10	Mucin 10, submandibular gland salivary mucin (200411, BC021401)	↓	
TTCTAAATCGGT	1925	282	0	0	1	0	0	0	0	0	3	0	0	0	0	0	2	PBSN	Probasin (8034, AF005204)	↓	
CCCAGTGTGTG	47	0	2	0	0	0	0	0	0	0	0	0	0	0	0	0	0	SVS1	Seminal vesicle secretion 1 (207324, NM_172888)	↓	↑S
GGCTCTGTTCT	261	72	0	0	0	1	0	1	0	0	0	0	0	2	0	0	1	SVP2	EST seminal vesicle protein 2 (1286, BB107209)	↓	↑S
ACCCAGACACG	193	1	0	0	0	1	0	0	0	0	0	0	0	0	0	0	0	SVS2	EST seminal vesicle protein, secretion 2 (99395, BB872622)	↓	↑S
AACCAACGATC	380	89	0	0	0	0	0	0	0	0	0	0	0	0	0	0	0	SVS2	EST seminal vesicle protein, secretion 2 (143501, BB123697)	↓	
ACCCACTCACA	24	1	0	0	0	0	0	1	0	0	0	0	0	0	0	0	0	SVS3	Seminal vesicle secretion 3 (260341, AF242220)	↓	↑S
GGGCCTAGAAA	2319	186	0	0	2	3	0	1	0	2	1	0	0	0	2	0	1	SVS5	Seminal vesicle secretion 5 (140154, NM 009301)	↓	↑C
GAAACTTGAAT	93	20	0	0	0	0	0	0	0	0	0	0	0	0	0	0	0	SVS5	EST seminal vesicle secretion 5 (140154, BB111962)	↓	
TCCTGAGGATG	42	11	0	0	0	0	0	0	0	0	0	0	0	0	0	0	0	SVS6	Seminal vesicle secretion 6 (3787, NM 013679)	↓	↑S
ATGGCCTGAGA	514	149	0	0	0	1	0	0	0	0	4	0	0	0	0	0	1	SVS7	Seminal vesicle protein, secretion 7 (99349, AF134204)	↓	↑S
TAITTTGCAAT	49	1	0	0	0	0	0	0	0	0	0	0	0	0	0	0	0	SVA	Seminal vesicle antigen (4119, NM 009299)	↓	↑S
ATGCAGTGGCG	414	3	0	0	0	0	0	0	0	0	0	1	0	0	0	0	0	SPINK3	Serine protease inhibitor, Kazal type 3 (272, AK007841)	↓	↑S
GGAGGTAGACC	614	42	0	0	1	1	0	0	0	0	0	0	0	0	0	0	0	TGM4	Transglutaminase 4 (prostate) (195309, AK035279)	↓	↑S

TABLE II. (Continued)

Tags	Prostate (14286)	Liver (16988)	Testis (56750)	Lung (159072)	Pituitary (126688)	Hypothalamus (165825)	Cerebral cortex (161045)	Femur (74763)	Skin (160828)	Male Fat (46057)	Male muscle (133398)	Female muscle (117944)	Female fat (150155)	Vagina (50724)	Ovary (5966)	Mammary gland (40411)	Uterus (178688)	Abbr	Description (UniGene, GenBank)	GDX	DHT
AAGACGGGTAG	91	1	0	0	0	0	0	0	0	0	0	0	0	0	0	0	0		No match	↓	↑S
ATCATCTTTAT	80	1	4	0	0	0	1	0	1	0	0	0	0	0	0	0	0		No match	↓	↑S
ACAAAACACAGA	77	4	0	0	0	0	0	0	0	0	0	0	0	0	0	0	0		No match	↓	↑S
CACCGGGCCTC	73	21	0	0	0	0	0	0	0	0	0	0	0	0	0	0	0		No match	↓	↑S
GAAAAGATAAAA	72	2	0	0	0	0	0	0	0	0	0	0	0	0	0	0	0		No match	↓	↑S
GCAACTAGCCT	66	1	0	0	0	0	0	0	0	0	0	0	0	0	0	0	0		No match	↓	↑S
ATATAAAGAG	59	12	0	0	0	0	0	0	0	0	0	0	0	0	0	0	0		No match	↓	↑S
GTGAGAAACAC	52	0	0	0	0	0	0	0	0	0	0	0	0	0	0	0	0		No match	↓	↑
GCACGTCAGAC	47	4	0	0	0	0	0	0	0	0	0	0	0	0	0	0	0		No match	↓	↑S
ATGGTTGTAAG	46	1	0	0	0	0	0	0	0	0	0	0	0	0	0	0	0		No match	↓	↑S
AACTCCGTCAT	45	4	0	0	0	0	0	0	0	0	0	0	1	0	0	0	0		No match	↓	↑S
TGTGAGCGACT	43	0	0	0	0	1	0	0	0	0	0	0	0	0	0	0	0		No match	↓	↑S
TATGGGTCCA	41	8	0	0	0	0	0	0	0	0	0	0	0	0	0	0	0		No match	↓	↑S
GGGCCTAAAAA	41	2	0	0	0	0	0	0	0	0	0	0	1	0	0	0	0		No match	↓	↑S
TTGTGGGGC	40	2	0	0	0	0	0	0	0	0	0	0	0	0	0	0	0		No match	↓	↑S
CTCAGAGCTCA	38	11	0	0	0	1	0	0	0	0	0	0	0	0	0	0	0		No match	↓	↑S
GGGAGAGTCC	35	7	0	0	0	0	0	0	0	0	0	0	0	0	0	0	0		No match	↓	↑S
AITTTAAAAAG	31	2	0	0	0	0	1	0	0	0	0	0	0	0	0	0	0		No match	↓	↑S
GAGGAATACAG	31	3	0	0	0	0	0	0	0	0	0	0	0	0	0	0	0		No match	↓	↑S
GGGCTAGAAT	31	4	0	0	0	0	0	0	0	0	0	0	0	0	0	0	0		No match	↓	↑S
GAGCCGTGGG	31	8	0	0	0	0	0	0	0	0	0	0	0	0	0	0	1		No match	↓	↑S
TAAAGTTTATAG	30	2	0	0	0	0	0	0	0	0	0	0	0	0	0	0	0		No match	↓	↑S
AAITGCAAACT	29	6	0	0	0	0	0	0	0	0	0	0	0	0	0	0	0		No match	↓	↑S
GCAAGGCTGGA	28	5	0	0	0	0	0	0	0	0	1	0	0	0	0	0	0		No match	↓	↑S
TTTTATTGCATT	25	1	0	0	0	0	0	0	1	0	0	0	3	0	0	2	2		No match	↓	↑S
GCAGAACCTGA	25	7	0	0	0	1	0	0	0	0	0	0	0	0	0	0	0		No match	↓	↑S
TGACTACTAGA	24	1	0	0	0	0	0	0	0	0	0	0	0	0	0	0	0		No match	↓	↑S
AITCTAGCTGT	24	1	0	0	0	0	0	0	0	0	0	0	0	0	0	0	0		No match	↓	↑S
ATGAGGGTGAG	24	0	0	0	0	0	1	0	0	0	0	0	0	0	0	0	0		No match	↓	↑S

GGCCTAGAAG	21	1	0	0	0	0	0	0	0	0	0	0	0	0	0	0	0	0	0	0	No match	→
TGGATGTTAG	21	3	0	0	0	0	0	0	0	0	0	0	0	0	0	0	0	0	0	0	No match	→
TCTGTATATGT	20	2	0	0	0	0	0	0	0	0	0	0	0	0	0	0	0	0	0	0	No match	→
AGATTIATTIA	20	5	0	0	0	1	0	0	0	0	0	0	0	0	0	0	0	0	0	0	No match	
GACACGGACAA	19	0	0	0	0	0	0	0	0	0	0	0	0	0	0	0	0	0	0	0	No match	

The numbers are tag numbers normalized to 100,000 tags sequenced in the SAGE libraries of each tissue. Abbr, abbreviation; GD_X, gonadectonized; DHT, dihydrotestosterone; C, common DHT-regulated gene (ARG); S, prostate tissue-specific ARG; Arrows show the significant effects of GD_X compared to intact group, or DHT compared to GD_X group on the gene expression level ($P \leq 0.05$).

proportion of cells in S phase while increasing apoptosis. On the other hand, HSPA5 gene expression after the transfection of HSPA5 siRNA was increased by 181%. Since there was a possibility of some compensation mechanisms, we measured the expression level at 24 hr after the transfection. As we expected, the expression level was down-regulated by 81.6% ± 0.7 (mean ± SD) at 24 hr after HSPA5 siRNA transfection compared to the negative control siRNA.

By comparing the SAGE libraries from each of the GD_X + DHT-treated tissues to the corresponding GD_X group, including adipose tissue, skeletal muscle, uterus and mammary gland, we found that most ARGs (81%) in the prostate were not regulated by DHT in other tissues. Only 22 out of 114 prostate ARGs were modulated by DHT commonly in at least two tissues (Table IV). These common DHT-responsive transcripts are involved in androgen receptor co-regulator, cytoskeleton assembly, protein expression and secretion, lipid metabolism, polyamine biosynthesis, immunity, and homeostasis.

DISCUSSION

The Most Abundant Transcripts in Prostate

To our knowledge, the present study is the first to report the most abundant transcripts, which encode proteins for prostatic secretion, polyamine transport, general energy metabolism, and immunity. Most of the functionally characterized transcripts were related to specialized prostatic secretion, such as probasin (PBSN), spermine binding protein (SBP), transglutaminase 4 (TGM4, also known as DP1), serine protease inhibitor Kazal type 3 (SPINK3) and several seminal vesicle fluid components (seminal vesicle protein 2: SVP2 and seminal vesicle protein secretion: SVS2/5/7) [19–23], which is consistent with the high-secretory activity of prostate as well as its role in the coagulation and spermatozoa transport.

Two mitochondrial transcripts involved in energy metabolism, namely ATP synthase F0 subunit 6 (ATP6) and cytochrome *c* oxidase subunit 3 (COX3), were abundantly expressed in the prostate. We have previously shown that mitochondrial transcripts are the most abundantly expressed in the high-energy expenditure tissues, such as skeletal muscle [6], uterus [7], cortex, and hypothalamus [8]. Since prostate is a muscular organ which contributes to controlling urine output and ejaculation, as well as exocrine and endocrine secretion [2], it is also highly energy-consuming. In addition, we found that a defensin family member, defensin beta 50 (DEFB50) was abundantly expressed in this tissue. Defensins are antimicrobial and cytotoxic peptides that influence membrane permeability and

TABLE III. Effects of HSPA5 and MAT2A siRNA on LNCaP Cell Growth and Interferon Response

	Control	HSPA5	MAT2A
HSPA5 mRNA expression	0.95 ± 0.11	2.69 ± 0.21*	—
MAT2A mRNA expression	0.95 ± 0.11	—	0.38 ± 0.17*
Cell cycle			
Apoptosis	2.57 ± 0.11	18.80 ± 2.33*	11.77 ± 4.42*
S-phase	0.72 ± 0.002	0.26 ± 0.04*	0.26 ± 0.05*
DNA contents	1.19 ± 0.04	0.84 ± 0.14*	0.42 ± 0.06*
IFIT2 mRNA expression	0.19 ± 0.08	0.21 ± 0.10	0.28 ± 0.24
IFIT3 mRNA expression	0.11 ± 0.04	0.10 ± 0.05	0.12 ± 0.10

Values are mean ± SD from triplicate measurements on three unique samples and expressed with a ratio to the mock transfection.

*Significantly different from control siRNA ($P < 0.05$).

chemotaxis as well as enhance innate host inflammatory defences against microbial invasion [24,25]. Although the biological function of DEFB50 is still unclear, a recent study already found DEFB50 abundantly and specifically expressed in the prostate and also proposed that DEFB50 contributes to prevent infectious disease within the prostate [11]. Furthermore, the current study revealed one RIKEN cDNA 9530002B09 and six novel transcripts abundantly expressed. It is surprising that these transcripts, which account for more than one-third of the top 20 most abundant transcripts, are still with uncharacterized function despite their extremely high expression levels. Taken together, the highly abundant transcripts involved in prostatic secretion, energy metabolism and immunity are a characteristic molecular signature of the prostate.

Tissue-Specific/Enriched Transcripts in the Prostate and Their Regulation by DHT

Transcripts expressed at significantly higher levels in the prostate than in other tissues were considered to be tissue specific/enriched. Many transcripts involved in the prostatic secretion, such as beta-microseminoprotein (BMSP, also known as prostate secretory proteins of 94 amino acids: PSP94, beta-inhibin and prostatic inhibin peptide: PIP), HSPA5, mucin 10 submandibular gland salivary mucin (MUC10), PBSN, SVS1/2/3/5/6/7, SVP2, seminal vesicle antigen (SVA), SPINK3, SBP and TGM4, were prostate-specific/enriched. Among these transcripts, PBSN, SVS2/5/7, SPINK3, SBP, and TGM4 were the most abundant transcripts in the prostate. Many transcripts encoding secretory products, such as MUC10 [26], TGM4 [27], SVSs and SVP2 [23], SVA [28,29] and SPINK3 [22], are related to spermatogenesis as well as sperm integrity and motility. In addition, 15 out of 16 transcripts in the prostatic

secretion were down-regulated by GDX, of which 10 transcripts were restored by DHT injection. GDX removes all testicular hormones, precursors and secreted factors as well as their interactions, whereas we administered only the most potent natural androgen, DHT, in GDX mice. Thus, this might explain the discrepancy of the effects of GDX or DHT in the transcripts regulated by only one of these experimental conditions.

Among all these transcripts involved in secretion, PSP94 is one of the three most abundant secretory proteins (PSP94, prostatic acid phosphatase: PAP and prostatic-specific antigen or gamma-seminoprotein: PSA) in the prostate gland [30], and PSP94 [31] and TGM4 [32] are well-known to be prostate-specific genes. Some previous studies have investigated prostate-specific genes. Srivastava's group compared 37 SAGE libraries and identified the prostate-specific/abundant transcripts in LNCaP cells, such as PSA, PSMA (prostate-specific membrane antigen), PAP and NK3 transcription factor related, locus 1 (NKX3.1) [33]. Another EST study in the normal prostate has shown that some genes, such as PBSN, SVA, SVP2, SVS2/3/6/7 and SBP, have enriched or restricted prostate expression [11]. Our wide-scale analysis verified most of these results and found new prostate tissue-specific/enriched transcripts such as HSPA5, SVS1/5 and SPINK3.

MAT2A is known to be widely distributed in many tissues [34–36]. However, our results show the preferential expression of MAT2A in the prostate. Moreover, the modulations by GDX and DHT were specific in the prostate. Since polyamines are crucial for growth and proliferation of mammalian cells and MAT2A promotes polyamine biosynthesis through catalysing the biosynthesis of *S*-adenosylmethionine, MAT2A could be a candidate regulating DHT-induced cell proliferation in the prostate. In addition, two transcripts of the

TABLE IV. Common ARGs in Prostate, Fat, Muscle, Uterus and Mammary Gland

Tags	Abbr	Description (UniGene, GenBank)	DHT effect						
			Prostate	Adipose tissue		Muscle		Uterus	Mammary gland
				Male	Female	Male	Female		
Androgen receptor co-regulator									
TCATCTTTAAC	CALR	Calreticulin (1971, AK075605)	↑		↓				
Cytoskeleton									
CACTGACCTCC	TPM2	Tropomyosin 2, beta (646, AK003186)	↑		↑		↓		
ACTGTCCGGGC	TNNT3	Troponin T3, skeletal, fast (350054, L48990)	↑		↑				
Protein expression									
GCCTTGGTGAA	EIF5A	Eukaryotic translation initiation factor 5A (196607, NM_181582)	↑				↑		
Protein secretion									
GGCCTAGAAA	SVS5	Seminal vesicle secretion 5 (140154, NM_009301)	↑				↑		
Lipid metabolism									
CAGGACTCCGT	SCD2	Stearoyl-Coenzyme A desaturase 2 (193096, M26270)	↑		↑				
Polyamine related cell proliferation									
TTGGTGGGACT	AMD1	S-Adenosylmethionine decarboxylase 1 (253533, NM_009665; 351410, XM_483892) and EST Transcribed locus (328446, AI552765)	↑				↑		
Immunity									
GTTCAAGTGAC	Ii	Ia-associated invariant chain (276499, NM_010545)	↓	↑					
Homeostasis									
GAAGAGGGGGA	HP	Haptoglobin (26730, NM_017370)	↓	↑					↑
No match									
ATTTTCAGTTT		No match	↓	↓	↓		↓	↓	↑
GAAAATGAGAA		No match	↓	↓	↓		↓	↓	↑
TCCTACAGTGG		No match	↓	↓	↓		↓	↓	↑
GAAAATGATAA		No match	↓	↓	↓		↓		
AATAAAGTTGT		No match	↓		↑			↓	
CATTGCCTTCA		No match	↓		↑				
AAATTAACAAG		No match	↓						
ACACATTATTT		No match	↓					↓	
TTTTTTTTTCCT		No match	↓		↑			↓	
GTAGGCACGGC		No match	↓					↑	
ACCCTCCTCCC		No match	↓						
ATTAAGAGGGA		No match	↓					↑	
ACCCGCCGGGC		No match	↓						↑

Abbr, abbreviation; DHT, dihydrotestosterone; Arrows show the significant effects of DHT compared to GDX group on the gene expression level ($P \leq 0.05$).

defensin beta family, DEFB50 and EST DEFB1, were preferentially expressed in the prostate. Since DEFB50 is a prostate tissue-enriched transcript which shows specific modulation by DHT in the prostate, future

functional studies of DEFB50 could be very useful in prostate gene targeting and hormonal therapy.

There are 47 other novel transcripts specifically/preferentially expressed in the prostate gland. Notably,

three novel transcripts (Tag sequences: CATG AAGA-CCGGTAG, GCAACTAGCCT and ATGGTTGTAAG) and one functionally uncharacterized transcript (RIKEN cDNA 9530002K18 gene) are prostate-specific transcripts and ARGs. To investigate the mechanisms underlying androgen regulation in the prostate, further characterization of these transcripts is needed.

It is interesting to note that many of the 79 prostate-specific/enriched transcripts, though much more highly induced in the prostate relative to the other organs, had fairly significant expression in the liver. As the largest gland in the human body, liver carries out many important functions in metabolism, detoxification as well as secretion. The prostate gland also secretes fluid, contributing the spermatozoa and ejaculation. Although the function of these secretory proteins such as PBSN, SVS5 and SVS7 in the liver is largely unknown, the results from the current study suggest overlapping secretory functions in the liver and prostate.

Tissue specificity can facilitate the pertinence of marker for diagnosis and therapy. Newly envisaged strategies utilize genes and proteins with prostate-specific/enriched expression for tissue-selective regimens incorporating vaccines, gene therapy, and siRNA as well as antibody-based cell targeting. In order to validate the role of tissue-specific ARGs in prostate cancer cell growth, we have selected genes specifically modulated by DHT in the prostate, among the prostate-specific/enriched transcripts, for the siRNA experiment in the LNCaP cells. The novel transcripts, as well as the genes encoding known secreted proteins or with a high signal peptide probability (≥ 0.9), were excluded since secreted proteins will also influence cells and tissues other than the target one. Thus, we selected two candidate genes, HSPA5 and MAT2A. Interestingly, a switch in expression from MAT1A to MAT2A has been reported to facilitate liver cancer growth [37]. Moreover, stress induction of HSPA5 plays a major role in unfold protein response (UPR) which contributes to tumor growth and confers drug resistance to cancer cells [38]. Furthermore, up regulation of HSPA5 is associated with the development of castration resistance [39]. Most importantly, this protein is expressed on the prostate cancer cell surface, which can be a functional molecular target for cancer treatment [40]. In the present study, HSPA5 and MAT2A siRNAs decreased cell proliferation and the proportion of cells in S phase while increasing apoptosis without interferon responses. Remarkably, 49% of cell population showed induction of apoptosis by HSPA5 siRNA. Although gene expression of HSPA5 was up-regulated at 96 hr after the transfection, the expression level after 24 hr was significantly reduced, by 82% of the negative control siRNA. These results suggest that cells which could induce HSPA5 gene expression survived until

96 hr after transfection. Taken together, these results validate the role of tissue-specific ARGs in prostate cancer cell growth, and suggest that the prostate-specific/enriched ARGs can be used as target for developing safe and effective treatment for prostate cancer.

Androgen-Regulated Transcripts Identified in at Least Two Tissues

Prostate is well known to be a highly androgen-dependent tissue, and androgens play very important roles in the development of prostate disease states such as benign hyperplasia and cancer. On the other hand, DHT also has various actions on many other tissues such as adipose tissue [41], skeletal muscle [42] and female genital organs [43]. Androgen has anabolic effect: Consistently, in the present study, almost all common ARGs of cytoskeleton, protein expression and secretion, polyamine biosynthesis in the prostate, skeletal muscle (male and female) and male adipose tissue were induced by DHT. On the other hand, tropomyosin 2 beta (TPM2) was decreased by DHT in female skeletal muscle. However, another isoform, TPM2, was induced by DHT [44]. In addition, androgen receptor co-regulators such as calreticulin (CALR) were reversely modulated by DHT in the prostate and female adipose tissue as well as two ARGs in immunity and homeostasis in the prostate and male adipose tissue. These aspects of these common and prostate-specific ARGs could be useful in efforts to retain the beneficial effects and avoid the side effects of DHT.

CONCLUSIONS

This study represents a global analysis of gene expression in the mouse prostate. Using SAGE strategy, we identified the most abundant and tissue-specific transcripts, providing sufficient evidence to characterize major and unique functions of the prostate. These results could serve as a resource for further studies of prostate development, physiology and pathology. Moreover, gene-based novel treatments such as targeting cytotoxic genes to prostate cancer cells using specific promoter as well as siRNA for prostate tissue-specific genes could lead to the development of a well-defined and highly specific anti-cancer treatment. In addition to known prostate-specific/enriched transcripts, newly identified transcripts in the current study such as HSPA5, SPINK3, SVS1/5 and MAT2A, as well as novel transcripts, could be potential targets for these new treatments. Indeed, we demonstrated that siRNAs against HSPA5 and MAT2A inhibited the growth of LNCaP cells. Finally, our findings on the effects of DHT on the prostate-specific/enriched transcripts, as well as common ARGs in several tissues,

provide a more complete understanding of DHT regulation. These results supply a molecular basis for the development of hormonal treatments with high effect and minimum side effects.

ACKNOWLEDGMENTS

We would like to thank Vincent Raymond, Claude Labrie, Van Luu-The, Ping Ye, Andrea Fournier, Yuichiro Nishida, and all principle investigators and research assistants involved in the ATLAS project. We also thank the Sequencing Facility and Q_RT-PCR Facility of Laval University Medical Centre for SAGE tag sequencing and Q_RT-PCR analyses. This work was supported by Genome Québec and Genome Canada.

REFERENCES

1. Thompson MIRaIM. Prostate physiology and regulation. Advanced therapy of prostate disease. Hamilton/London: BC Decker Inc.; 2000. pp 92–117.
2. Kumar VL, Majumder PK. Prostate gland: Structure, functions and regulation. *Int Urol Nephrol* 1995;27(3):231–243.
3. Velculescu VE, Zhang L, Vogelstein B, Kinzler KW. Serial analysis of gene expression. *Science* 1995;270(5235):484–487.
4. Dinel S, Bolduc C, Belleau P, Boivin A, Yoshioka M, Calvo E, Piedboeuf B, Snyder EE, Labrie F, St-Amand J. Reproducibility, bioinformatic analysis and power of the SAGE method to evaluate changes in transcriptome. *Nucleic Acids Res* 2005; 33(3):e26.
5. St-Amand J, Okamura K, Matsumoto K, Shimizu S, Sogawa Y. Characterization of control and immobilized skeletal muscle: An overview from genetic engineering. *FASEB J* 2001;15(3):684–692.
6. Yoshioka M, Tanaka H, Shono N, Snyder EE, Shindo M, St-Amand J. Serial analysis of gene expression in the skeletal muscle of endurance athletes compared to sedentary men. *FASEB J* 2003;17(13):1812–1819.
7. Larose M, St-Amand J, Yoshioka M, Belleau P, Morissette J, Labrie C, Raymond V, Labrie F. Transcriptome of mouse uterus by serial analysis of gene expression (SAGE): Comparison with skeletal muscle. *Mol Reprod Dev* 2004;68(2):142–148.
8. Nishida Y, Yoshioka M, St-Amand J. The top 10 most abundant transcripts are sufficient to characterize the organs functional specificity: Evidences from the cortex, hypothalamus and pituitary gland. *Gene* 2005;344:133–141.
9. Bolduc C, Larose M, Lafond N, Yoshioka M, Rodrigue MA, Morissette J, Labrie C, Raymond V, St-Amand J. Adipose tissue transcriptome by serial analysis of gene expression. *Obes Res* 2004;12(5):750–757.
10. Ye P, Yoshioka M, Gan L, St-Amand J. Regulation of global gene expression by ovariectomy and estrogen in female adipose tissue. *Obes Res* 2005;13(6):1024–1030.
11. Abbott DE, Pritchard C, Clegg NJ, Ferguson C, Dumpit R, Sikes RA, Nelson PS. Expressed sequence tag profiling identifies developmental and anatomic partitioning of gene expression in the mouse prostate. *Genome Biol* 2003;4(12):R79.
12. Ma C, Yoshioka M, Boivin A, Labrie F, St-Amand J. Atlas of dihydrotestosterone actions on the transcriptome of prostate *in vivo*. In: Proceeding of 2005 Annual Meeting of the Canadian Physiological Society. 2005; Quebec. p 27.
13. Howell S, Shalet S. Testosterone deficiency and replacement. *Horm Res* 2001;56 (Suppl 1):86–92.
14. Velculescu VE, Zhang L, Zhou W, Vogelstein J, Basrai MA, Bassett DE, Jr., Hieter P, Vogelstein B, Kinzler KW. Characterization of the yeast transcriptome. *Cell* 1997;88(2):243–251.
15. Kenzelmann M, Muhlemann K. Substantially enhanced cloning efficiency of SAGE (Serial Analysis of Gene Expression) by adding a heating step to the original protocol. *Nucleic Acids Res* 1999;27(3):917–918.
16. Adams MD, Kerlavage AR, Fleischmann RD, Fuldner RA, Bult CJ, Lee NH, Kirkness EF, Weinstock KG, Gocayne JD, White O, et al. Initial assessment of human gene diversity and expression patterns based upon 83 million nucleotides of cDNA sequence. *Nature* 1995;377(6547 Suppl):3–174.
17. Luu-The V, Paquet N, Calvo E, Cumps J. Improved real-time RT-PCR method for high-throughput measurements using second derivative calculation and double correction. *Biotechniques* 2005;38:287–293.
18. Lash AE, Tolstoshev CM, Wagner L, Schuler GD, Strausberg RL, Riggins GJ, Altschul SF. SAGEmap: A public gene expression resource. *Genome Res* 2000;10(7):1051–1060.
19. Matuo Y, Adams PS, Nishi N, Yasumitsu H, Crabb JW, Matusik RJ, McKeehan WL. The androgen-dependent rat prostate protein, probasin, is a heparin-binding protein that co-purifies with heparin-binding growth factor-1. *In Vitro Cell Dev Biol* 1989;25(6):581–584.
20. Mills JS, Needham M, Parker MG. Androgen regulated expression of a spermine binding protein gene in mouse ventral prostate. *Nucleic Acids Res* 1987;15(19):7709–7724.
21. Wilson EM, French FS. Biochemical homology between rat dorsal prostate and coagulating gland. Purification of a major androgen-induced protein. *J Biol Chem* 1980;255(22):10946–10953.
22. Mills JS, Needham M, Parker MG. A secretory protease inhibitor requires androgens for its expression in male sex accessory tissues but is expressed constitutively in pancreas. *EMBO J* 1987;6(12):3711–3717.
23. Aumuller G, Seitz J. Protein secretion and secretory processes in male accessory sex glands. *Int Rev Cytol* 1990;121:127–231.
24. Yang D, Biragyn A, Kwak LW, Oppenheim JJ. Mammalian defensins in immunity: More than just microbicidal. *Trends Immunol* 2002;23(6):291–296.
25. Sawicki W, Mystkowska ET. Contraceptive potential of peptide antibiotics. *Lancet* 1999;353(9151):464–465.
26. Xu R, Cai J, Xu T, Zhou W, Ying B, Deng K, Zhao S, Li C. Molecular cloning and mapping of a novel ADAM gene (ADAM29) to human chromosome 4. *Genomics* 1999;62(3): 537–539.
27. Williams-Ashman HG. Transglutaminases and the clotting of mammalian seminal fluids. *Mol Cell Biochem* 1984;58(1–2):51–61.
28. Huang YH, Chu ST, Chen YH. Seminal vesicle autoantigen, a novel phospholipid-binding protein secreted from luminal epithelium of mouse seminal vesicle, exhibits the ability to suppress mouse sperm motility. *Biochem J* 1999;343(Pt 1):241–248.
29. Huang YH, Chu ST, Chen YH. A seminal vesicle autoantigen of mouse is able to suppress sperm capacitation-related events stimulated by serum albumin. *Biol Reprod* 2000;63(5):1562–1566.

30. Abrahamsson PA, Lilja H. Three predominant prostatic proteins. *Andrologia* 1990;22 (Suppl 1):122–131.
31. Thota A, Karajgikar M, Duan W, Gabriel MY, Chan FL, Wong YC, Sakai H, Chin JL, Moussa M, Xuan JW. Mouse PSP94 expression is prostate tissue-specific as demonstrated by a comparison of multiple antibodies against recombinant proteins. *J Cell Biochem* 2003;88(5):999–1011.
32. Dubbink HJ, de Waal L, van Haperen R, Verkaik NS, Trapman J, Romijn JC. The human prostate-specific transglutaminase gene (TGM4): Genomic organization, tissue-specific expression, and promoter characterization. *Genomics* 1998;51(3):434–444.
33. Xu LL, Su YP, Labiche R, Segawa T, Shanmugam N, McLeod DG, Moul JW, Srivastava S. Quantitative expression profile of androgen-regulated genes in prostate cancer cells and identification of prostate-specific genes. *Int J Cancer* 2001;92(3):322–328.
34. Kotb M, Mudd SH, Mato JM, Geller AM, Kredich NM, Chou JY, Cantoni GL. Consensus nomenclature for the mammalian methionine adenosyltransferase genes and gene products. *Trends Genet* 1997;13(2):51–52.
35. Horikawa S, Tsukada K. Molecular cloning and developmental expression of a human kidney S-adenosylmethionine synthetase. *FEBS Lett* 1992;312(1):37–41.
36. Alvarez L, Corrales F, Martin-Duce A, Mato JM. Characterization of a full-length cDNA encoding human liver S-adenosylmethionine synthetase: Tissue-specific gene expression and mRNA levels in hepatopathies. *Biochem J* 1993;293(Pt 2):481–486.
37. Cai J, Mao Z, Hwang JJ, Lu SC. Differential expression of methionine adenosyltransferase genes influences the rate of growth of human hepatocellular carcinoma cells. *Cancer Res* 1998;58(7):1444–1450.
38. Li J, Lee AS. Stress induction of GRP78/BiP and its role in cancer. *Curr Mol Med* 2006;6(1):45–54.
39. Pootrakul L, Datar RH, Shi SR, Cai J, Hawes D, Groshen SG, Lee AS, Cote RJ. Expression of stress response protein Grp78 is associated with the development of castration-resistant prostate cancer. *Clin Cancer Res* 2006;12(20 Pt 1):5987–5993.
40. Arap MA, Lahdenranta J, Mintz PJ, Hajitou A, Sarkis AS, Arap W, Pasqualini R. Cell surface expression of the stress response chaperone GRP78 enables tumor targeting by circulating ligands. *Cancer Cell* 2004;6(3):275–284.
41. Mayes JS, Watson GH. Direct effects of sex steroid hormones on adipose tissues and obesity. *Obes Rev* 2004;5(4):197–216.
42. Herbst KL, Bhasin S. Testosterone action on skeletal muscle. *Curr Opin Clin Nutr Metab Care* 2004;7(3):271–277.
43. Traish AM, Kim N, Min K, Munarriz R, Goldstein I. Role of androgens in female genital sexual arousal: Receptor expression, structure, and function. *Fertil Steril* 2002;77 (Suppl 4):S11–S18.
44. Yoshioka M, Boivin A, Bolduc C, St-Amand J. Gender difference of androgen actions on skeletal muscle transcriptome 2007;39(2):119–133.